Radiation-Induced Microbleeds after Cranial Irradiation: Evaluation by Phase-Sensitive Magnetic Resonance Imaging with 3.0 Tesla

Tomohiko Tanino,* Yoshiko Kanasaki,* Takatoshi Tahara,* Koichi Michimoto,* Kazuhiko Kodani,* Suguru Kakite,* Toshio Kaminou,* Takashi Watanabe† and Toshihide Ogawa*

**Division of Radiology, Department of Pathophysiological and Therapeutic Science, School of Medicine, Tottori University Faculty of Medicine, Yonago 683-8504, Japan and †Division of Neurosurgery, Department of Brain and Neurosciences, School of Medicine, Tottori University Faculty of Medicine, Yonago 683-8504, Japan*

ABSTRACT

Background Although there are many reports regarding radiation-induced microbleeds, its frequency, relation to dose and latency after radiation are not fully elucidated. The purpose of this study was to evaluate the frequency, latency, patient factors and dose relation of radiation-induced microbleeds after cranial irradiation using phase-sensitive magnetic resonance imaging (PSI) at 3.0 T.

Methods Retrospective evaluation of 34 patients (age range, 13–78 years; mean, 49 years; follow-up period, 3–169 months; mean 29 months) who had undergone cranial irradiation using magnetic resonance (MR) imaging including PSI was performed. Twenty-three patients received high-dose irradiation (44–60 Gy), and 11 patients received 24–30 Gy whole brain irradiation. When microbleeds were detected on MR imaging in these high-dose irradiation patients, dose distribution maps were reproduced by reviewing the clinical records. Then the irradiated areas were divided into 6 radiation-dose classes: regions > 55 Gy, 45–55 Gy, 35–45 Gy, 25–35 Gy, 15–25 Gy and 5–15 Gy. The frequency of microbleeds in each radiation-dose class was analyzed.

Results Microbleeds were detected in 7 (21%) of 34 patients on T2-weighted imaging, whereas they were detected in 16 (47%) of the 34 patients on PSIs. The frequency of microbleeds was higher than previously reported. The latency of radiation-induced microbleeds after radiation was 3 months to 9 years (mean, 33 months). In high-dose irradiation patients, the frequency of microbleeds significantly was associated with radiation dose. There were no foci that were observed in regions that had received < 25 Gy.

Conclusion Radiation-induced microbleeds occurred more frequently in the present study than has been previously reported. PSI can be used to detect these vascular changes earlier than other conventional MR imaging techniques.

Key words cranial irradiation; magnetic resonance imaging; radiation injury

Radiation therapy is an efficacious treatment for brain neoplasms. However, cranial irradiation can cause complications as well as benefits. Complications of cranial irradiation include necrosis, diffuse white matter injury, central nervous system atrophy, mineralization, microangiopathy, telangiectasia, optic neuropathy, and large vessel vasculopathy.[1] Although clinically important complications are infrequent with modern radiation therapy techniques, asymptomatic complications following radiation therapy, such as diffuse white matter injury, central nervous system atrophy, and vascular injury, can be present by follow-up computed tomography (CT) and magnetic resonance (MR) imaging. Radiation-induced vascular injury can be classified into 2 types: large arterial injury and telangiectasia, or cryptic vascular malformation. Radiation-induced telangiectasia in the brain results in varying amounts of hemorrhage and may have an appearance similar to that of cryptic vascular malformation.[2] These lesions are usually small and can be mixed with cavernous malformation. As the differentiation of these small lesions is often difficult on MR imaging, we refer to these conditions as radiation-induced microbleeds. Although there have been many reports concerning radiation-induced microbleeds in the past, the frequency, dose relation, and latency of radiation-induced microbleeds are not fully elucidated.

MR imaging is useful for diagnosis and evaluation of these cerebral complications following radiation therapy.[3] MR imaging is currently considered to be the best imaging technique for evaluation of brain injury following radiation therapy.[4] Susceptibility-weighted imaging (SWI) is a 3-dimensional gradient echo MR imaging technique using the blood oxygen level-dependent

Corresponding author: Tomohiko Tanino
t.tanino@med.tottori-u.ac.jp
Received 2012 December 4
Accepted 2012 December 13
Abbreviations: CT, computed tomography; FA, flip angle; FLAIR, fluid attenuated inversion recovery; FOV, field of view; FSE, fast spin echo; FSPGR, fast spoiled gradient recalled acquisition in steady state; MR, magnetic resonance; PSI, phase-sensitive magnetic resonance imaging; SWI, susceptibility-weighted imaging; TE, echo time; TI, inversion time; TR, repetition time

effect.[5] SWI is highly sensitive to differences of the magnetic susceptibility properties between tissues, such as blood products (including deoxyhemoglobin, methemoglobin and hemosiderin). T2*-weighted imaging is also considered to be a highly sensitive MR technique for visualization of cerebral hemorrhage. However, SWI is currently considered to be more sensitive than other conventional MR imaging techniques, including T2*-weighted imaging, for detection of hemorrhage.[6] Phase-sensitive MR imaging (PSI), based on principles similar to those of SWI, is obtained by multiplication of the phase and magnitude images using Windows-based software.

The purpose of this study was to evaluate the frequency, latency, patient factors, and dose relation of radiation-induced microbleeds after cranial irradiation using PSI, and to evaluate the usefulness of PSI for detection of radiation-induced microbleeds.

MATERIALS AND METHODS

Patients

MR imaging and clinical records of 34 patients (18 men and 16 women; age range, 13–78 years; mean age, 49 years) who had undergone brain irradiation and undergone MR imaging including PSI with a follow-up period of at least 3 months were retrospectively reviewed. The average follow-up period was 29 months (3–169 months). Eleven patients received 24–30 Gy of whole brain irradiation. Eight of these patients had been diagnosed with brain metastases, 1 had been diagnosed with germinoma by biopsy, and 2 had received prophylactic cranial irradiation for lung small cell carcinoma. Twenty-two patients received 44–60 Gy of localized brain irradiation, and 1 patient received 60 Gy of opposing portal irradiation. These patients had undergone surgical resection or biopsy and diagnoses proved by their pathological diagnosis. The diagnoses included 17 high-grade gliomas, 2 central neurocytomas, 1 medulloblastoma, 1 meningioma, 1 germinoma and 1 metastasis from occult primary cancer. When microbleeds were detected on MR imaging in patients who had received high-dose irradiation (44–60 Gy), dose distribution maps were reproduced by reviewing clinical records. Then, the area that had received irradiation was divided into 6 radiation-dose classes: regions with > 55 Gy, 45–55 Gy, 35–45 Gy, 25–35 Gy, 15–25 Gy and 5–15 Gy. One patient who received 60 Gy of opposing portal irradiation was regarded to have received > 55 Gy. Microbleeds were then evaluated in each radiation-dose class region.

All 34 patients were divided into 2 groups by factors such as gender (male versus female), age (over 60 years versus less than 60 years), hypertension (with versus without), and chemotherapy (done versus not done). Patient characteristics are summarized in Table 1. Age is defined as the patient's age at the beginning of the irradiation. Patients who had received medication for hypertension were classified as having hypertension.

Table I. Patient characteristics

Number of patients		34
Gender	Male	18
	Female	16
Age (yr)	Range	13–78
	Mean	49
	Median	51
	60 and over	12
	Less than 60	22
Follow-up period (mo)	Range	3–169
	Average	29
Irradiation	Localized irradiation	22
	Opposing portal irradiation	1
	Whole brain irradiation	11
Total dose (Gy)	Localized irradiation	44–60
	Opposing portal irradiation	60
	Whole brain irradiation	24–30
Number of fractions	Localized irradiation	22–30
	Opposing portal irradiation	30
	Whole brain irradiation	10–12
Diagnosis	High-grade gliomas	17
	Central neurocytomas	2
	Germinoma	2
	Medulloblastoma	1
	Meningioma	1
	Metastasis from occult primary cancer	1
	Brain metastases	8
	Prophylactic cranial irradiation for lung small cell carcinoma	2
Chemotherapy	Done	30
	Not done	4
Hypertension	Patient with hypertension	4
	Patient without hypertension	30
Serial imaging	Available	21
	Not available	13

Brain radiation therapy

Eleven patients who received whole brain irradiation were treated with total doses between 24–30 Gy, at 2.0–3.0 Gy dose per fraction. The treatment duration was 2–2.4 weeks. The other 23 patients were treated with total doses between 44–60 Gy, at a dose of 1.8–2.0 Gy per fraction. The treatment duration was 4.4–6 weeks. A 6 MV-Xray was used (Clinic iX 4217, Varian Medical Systems, Palo Alto, CA; or Linac EXL-15SP Mitsubishi Electric, Tokyo, Japan) in all patients.

MR imaging

Before and at least 3 months after completion of radiation therapy, all patients underwent MR imaging. All

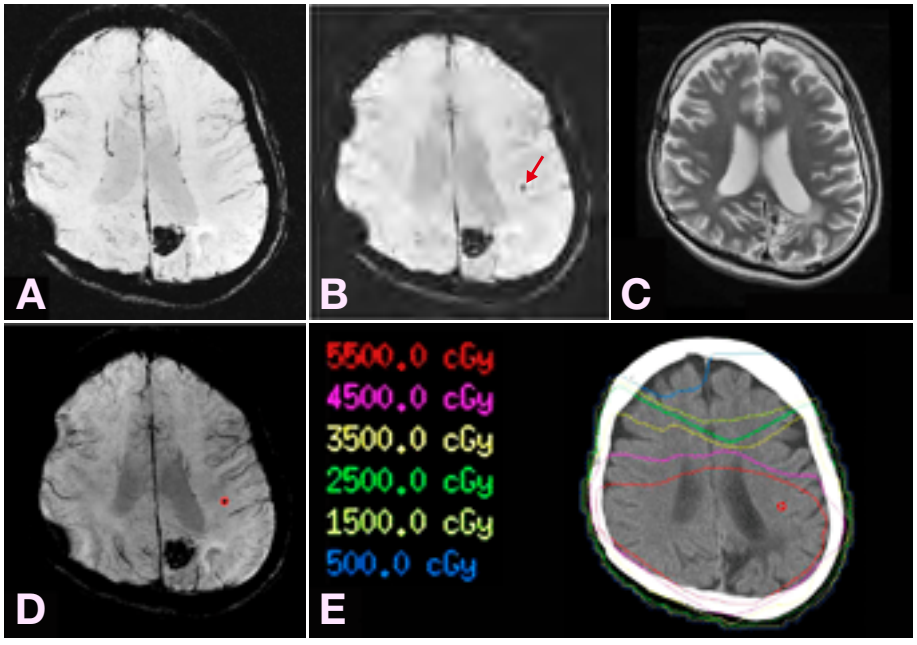

Fig. 1. A 31-year-old man with surgical resection of a high-grade glioma in the left parietal lobe, which was followed by localized irradiation at a dose of 60 Gy.

A: PSI obtained 17 months after completion of radiation therapy.

B: PSI obtained 33 months after completion of radiation therapy. A hypointense focus that cannot be detected in **A** appears in the left parietal white matter in **B** (arrow). This focus can be interpreted as microbleed.

C: T2-weighted image obtained 33 months after completion of radiation therapy. The microbleed detected in **B** cannot be detected.

D: Fused PSI image. The microbleed is contoured.

E: Reproduced dose distribution map. The microbleed is recognized in regions with > 55 Gy.

PSI, phase-sensitive magnetic resonance imaging.

MR brain images were obtained at 3.0 T (Signa EXCITE HD, General Electric, Milwaukee, WI) using an 8-channel phased-array coil (USA Instruments, Aurora, OH), except for 1 patient. That patient was examined at 1.5 T (Symphony, Siemens, Germany) prior to radiation therapy and was examined with the 3.0 T MR system mentioned above after radiation therapy. At 3.0 T, we obtained axial T1-weighted images with and without intravenous gadopentetate dimeglumine (Magnevist; Bayer, Osaka, Japan) using a fast spoiled gradient recalled acquisition in steady state (FSPGR) sequence, T2-weighted fast spin echo (FSE) images, and fluid attenuated inversion recovery (FLAIR) images. The imaging parameters were as follows: FSPGR, repetition time (TR)/echo time (TE) of 9/2 ms, flip angle (FA) of 13˚, 512 × 256 matrix, 1 excitation, 21 cm field of view (FOV), bandwidth of 122 Hz/pixel and a slice thickness of 1.4 mm without intersection gap; T2-weighted FSE, TR/TE of 4000/95 ms, 512 × 320 matrix, 21 cm FOV, section thickness/intersection gap of 5/1.5 mm; and FLAIR, TR/TE/inversion time (TI) of 10,000/116/2500 ms, 384 × 192 matrix, 21 cm FOV and a section thickness/intersection gap of 5/1.5 mm. At 1.5 T, T1-weighted images with and without contrast medium, T2-weighted images, and FLAIR images were obtained using similar sequences.

PSI, on the basis of principles similar to those of SWI,[7] was acquired after the radiation therapy using a 3-dimensional-spoiled gradient recalled acquisition steady state sequence with flow compensation using the following imaging parameters: TR/TE of 45/30 ms, FA of 20˚, FOV of 21 cm, 512 × 192 matrix, section thickness of 1.5 mm and an acquisition time of 7 min 40–50 s. All images were obtained in the axial plane. PSI were post-processed using a high-pass filter and then the images were converted into negative phase masks that were multiplied 4 times into the corresponding magnitude images using research software (PSIRecon: GE Yokogawa Medical Systems, Tokyo). A minimum intensity projection was performed to display the processed data using contiguous 10-mm-thick sections with 7-mm overlap in the axial plane. The follow-up interval for the MR imaging was dependent on the clinical course, and serial MR images including PSI were obtained in 21 patients after radiation therapy.

Image evaluation

Microbleeds were determined to be present if a small focus of very low signal-intensity was recognized on PSI

and/or T2-weighted imaging. The presence or absence of microbleeds was evaluated by 2 experienced neuroradiologists. Areas of surgical intervention and calcifications were excluded by reviewing surgical records and subsequent CT performed within 1 month from MR imaging. Regions of metastasis or residual tumor were excluded by the combined inspection of T1-weighted images and contrast enhanced T1-weighted images. In cases with microbleeds found on MR imaging performed only once after radiation therapy, previously existing microbleeds (prior to irradiation) were excluded through comparison of previous MR images with MR images including PSI after radiation therapy. The final decision regarding the presence of microbleeds on MR imaging was made by means of mutual consent between 2 neuroradiologists. In patients who had received high-dose irradiation and who had detected microbleeds, PSI was fused to the dose distribution map. Then, the microbleed was evaluated in each radiation-dose class region.

Statistical analyses

To compare the detection rate of PSI and T2-weighted imaging, the Fisher exact test was used. The Fisher exact test was used for comparisons between the groups, which were divided by several factors (including gender, age, hypertension and chemotherapy). In patients with microbleed in the high-dose irradiation group, Cochran-Armitage trend test was used to identify appearance of microbleed associated with radiation dose. A P value < 0.05 was considered to indicate statistical significance.

RESULTS

Microbleeds were detected in 7 (21%) of 34 patients on T2-weighted imaging, whereas they were detected in 16 (47%) of the 34 patients on PSIs. A typical case of microbleed is shown in Fig. 1. There was a significant difference in detection of microbleeds in PSIs and T2-weighted images (P = 0.039, Fisher exact test). Microbleeds were found in 12 patients in the high-dose irradiation group, while they were found in 4 patients in the whole brain irradiation group. Five patients had 1 focus, and the other 11 patients had 2 or more foci. There were 45 foci in 15 patients, except 1 patient who had too many foci to count. Of the 16 patients with microbleeds, the appearance of microbleed was detected on the 2nd and/or 3rd follow-up PSI after radiation therapy in 11 patients. In the remaining 5 patients, the appearance of microbleed was detected on the 1st PSI after radiation therapy. The 2 neuroradiologists concluded that these microbleeds developed after the radiation therapy on the basis of detailed comparison of T2-weighted images before and after radiation therapy and PSI after radiation therapy. No microbleeds disappeared during 3 to 169 months after the end of radiation therapy.

Table 2. Results of comparison between groups divided by several factors

	Number of patients			
	Total	With microbleeds	Without microbleeds	P value
Gender				0.74†
Male	18	9	9	
Female	16	7	9	
Age*				0.29†
60 and over	12	4	8	
Less than 60	22	12	10	
Chemotherapy				0.60†
Done	30	15	15	
Not done	4	1	3	
Hypertension				1†
With	4	2	2	
Without	30	15	15	

*yr.
†No significant difference between 2 groups with Fisher's exact test.

In the present study the latency period for radiation-induced microbleeds was 3 months to 9 years. The mean and median latency periods in which microbleeds were first observed were 33 months and 19 months, respectively. In 27 patients that were examined by PSI within 2 years after radiation therapy, microbleeds were detected in 10 patients (37%).

There was no statistically significant difference in the frequency of microbleeds between the groups, which were divided by gender (P = 0.74), age (P = 0.29), hypertension (P = 1.0) and chemotherapy (P = 0.60). Results of comparison of each group are summarized in Table 2. In 23 patients who received high-dose irradiation of 44–60 Gy, 12 patients developed microbleeds. In these 12 patients, frequency of microbleeds was significantly associated with radiation dose (P < 0.001, Cochran-Armitage trend test). The frequency of microbleeds according to the dose class is summarized in Table 3. No

Table 3. Results from 12 patients with high-dose irradiation with microbleeds according to radiation-dose classes

Radiation dose class (Gy)	Number of regions	Number of regions with microbleeds	Frequency of microbleeds (%)
Over 55	8	6	75
45–55	11	7	63.6
35–45	11	3	27.2
25–35	11	3	27.2
15–25	11	0	0
5–15	11	0	0

foci were observed in the regions that had received < 25 Gy irradiation.

DISCUSSION

The mechanism of radiation-induced brain injury is not yet fully understood.[8] There is a considerable literature regarding the pathogenesis of such side effects. Various hypotheses emphasize vascular changes, a direct effect on glial cells and/or an immunological mechanism.[9]

A mechanism for vascular injury is as follows. In acute vascular injury, transient vasodilatation occurs with variable changes in capillary permeability that sometimes manifests as vasogenic edema.[10.11] Changes in capillary permeability in response to radiation therapy to the central nervous system have been quantitated and found to entail specific variability in molecular sizes.[12.13] In chronic radiation-induced injury such as endothelial damage, vascular ectasia and microbleeds can occur. These changes result in increased capillary permeability at the site of vascular injury with resultant cytotoxic and vasogenic edema. Progressive vascular changes include vessel wall thickening with consequent thrombosis, infarction and necrosis.[11] Results of these studies provide support for the concept that vascular injury plays a pivotal role in the development of radiation-induced brain injury.

As noted above, radiation-induced vascular injury commonly affects small arteries and capillaries.[14] In addition, less commonly progressive radiation-induced large vessel vasculopathy may occur. Intracerebral hemorrhage occasionally occurs as a late delayed reaction.[15] In an animal study, vascular abnormalities were shown to occur before the development of parenchymal changes in the brain.[16] Therefore, radiation-induced vascular alterations, as represented by microbleeds, should be evaluated in order to know the severity of brain injury.

The frequency of radiation-induced telangiectasia has been reported to be 20%.[17] The frequency of radiation-induced microbleeds in the present study was higher than the frequency of telangiectasia, despite the short follow-up period. As PSI was acquired only once in the 5 patients with microbleeds, there is a possibility that the present study included patients with previously existing microbleeds. However, even after taking this possibility into account, the frequency is still higher than that of the previous reports. This may be because PSI is a highly sensitive technique for visualization of cerebral hemorrhage. SWI and PSI are currently recognized to be more sensitive than the other conventional MR imaging techniques for detection of hemorrhage.[6] In many previous reports, microbleeds were detected mainly in T2-weighted images. Therefore, many microbleeds might have been overlooked. In fact, the frequency of microbleeds in the present study in T2-weighted images was similar to the frequency of telangiectasia in previous reports. Therefore, it could be concluded that radiation-induced microbleeds occur more frequently than has been previously assumed.

The latency period of radiation-induced microbleeds has been reported on numerous occasions to have a wide range, between 5 months and 22 years.[1] In the present study, the latency period was 3 months to 9 years. The latency period in the present study is similar to previous reports, but in general in the present study microbleeds appeared relatively early. Lupo et al recently reported using SWI with 7 T that 2 patients developed microbleed in the 5 patients within 2 years after radiation therapy.[18] In the present study, 10 patients developed microbleeds in the 27 patients within 2 years after radiation therapy. This early appearance may be related to the high sensitivity of PSI.

In general, complications of radiation therapy to the brain are dependent on total dose, patient age, underlying disease and concomitant therapy.[3] Patient factors such as gender, age, hypertension and chemotherapy seem to be unrelated to the appearance of telangiectasia. However, it is known that the immature brain is more sensitive to radiation than the adult brain.[19] Koike et al. reported that radiation-induced telangiectasia occurs more frequently in younger patients.[17] In the present study there were only 3 patients whose age was under 20 years. If more pediatric patients were included, a significant difference might have been seen. Investigation of a larger number of younger patients is therefore desired.

To our knowledge, there have been no reports that have proven a dose predominance in radiation-induced microbleeds. In order to investigate the relationship between microbleeds and radiation dose, the irradiation areas were separated into 6 regions according to the radiation dose in 12 patients who received high-dose radiation with microbleeds. Frequency of microbleeds was significantly associated with radiation dose in the present report. In previous reports, telangiectasias have developed in patients who received radiation doses ranging from 18 to 78 Gy.[2, 20] In the present study there were no foci that were observed in regions that had received less than 25 Gy. The radiation dose threshold for development of microbleed is still not clear. To our knowledge, there is no report of radiation-induced microbleed with a dose lower than 18 Gy. With low radiation doses, microbleed may be less likely to develop. However, the present report suggests that vascular injury may occur around 25 Gy. PSI can be used to detect these vascular changes

earlier than other conventional MR imaging techniques.

There are several limitations to the present study. First, this study lacks histopathologic confirmation of all cases. Second, PSI before irradiation was not available; however, exclusion of calcification and microbleeds before irradiation was attempted in comparing previous MR and subsequent CT images. Lastly, the short observation period and the irradiation volume effect were not taken into consideration.

The authors declare no conflict of interest.

REFERENCES

1 Rabin BM, Meyer JR, Berlin JW, Marymount MH, Palka PS, Russell EJ. Radiation-induced changes in the central nervous system and head and neck. Radiographics. 1996;16:1055-72. PMID: 8888390.

2 Gaensler EH, Dillon WP, Edwards MS, Larson DA, Rosenau W, Wilson CB. Radiation-induced telangiectasia in the brain simulates cryptic vascular malformations at MR imaging. Radiology. 1994;193:629–36. PMID: 7972799.

3 Valk PE, Dillon WP. Radiation Injury of the brain. AJNR Am J Neuroradiol. 1991;12:45-62. PMID: 7502957.

4 Pružincová L, Šteņo J, Srbecký M, Kalina P, Rychlý B, Bolješíková E, et al. MR imaging of late radiation therapy- and chemotherapy-induced injury: a pictorial essay. Eur Radiol. 2009;19:2716-27. PMID: 19471942.

5 Haacke EM, Xu Y, Cheng YC, Reichenbach JR. Susceptibility weighted imaging (SWI). Magn Reson Med. 2004;52:612-8. PMID: 15334582.

6 Mori N, Miki Y, Kikuta K, Fushimi Y, Okada T, Urayama S, et al. Microbleeds in moyamoya disease: susceptibility-weighted imaging versus T2* weighted imaging at 3 tesla. Invest Radiol. 2008;43:574-9. PMID: 18648257.

7 Fujii S, Kanasaki Y, Matsusue E, Kakite S, Kminou T, Ogawa T. Demonstration of cerebral venous variations in the region of the third ventricle on phase-sensitive imaging. AJNR Am J Neuroradiol. 2010;31:55-9. PMID: 19729543.

8 Belka C, Budach W, Kortmann RD, Bamberg M. Radiation induced CNS toxicity-molecular and cellular mechanisms. Br J Cancer. 2001;85:1233-9. PMID: 11720454.

9 Sheline GE, Wara WM, Smith V. Therapeutic irradiation and brain injury. Int J Radiat Oncol Biol Phys. 1980;6:1215-28. PMID: 7007303.

10 Husain MM, Garcia JH. Cerebral "radiation necrosis": vascular and glial features. Acta Neuropathol. 1976;36:381-5. PMID: 1015244.

11 Burger PC, Boyko OB. The pathology of central nervous system radiation injury. In: Gutin PH, Leibel SA, Sheline GE, eds. Radiation injury to the nervous system. New York: Raven Press; 1991. p. 191-208.

12 Levin VA, Edwards MS, Byrd A. Quantitative observations of the acute effects of X-irradiation on brain capillary permeability: Part I. Int J Radiat Oncol Biol Phys. 1979;5:1627-31. PMID: 94058.

13 Edwards MS, Levin VA, Byrd A. Quantitative observations of the subacute effects of X irradiation on brain capillary permeability: Part II. Int J Radiat Oncol Biol Phys. 1979;5:1633-5. PMID: 536271.

14 Roth NM, Sontag MR, Kiani MF. Early effects of ionizing radiation on the microvascular networks in normal tissue. Radiat Res. 1999;151:270-7. PMID: 10073664.

15 Chung E, Bodensteiner J, Hogg JP. Spontaneous intracerebral hemorrhage: a very late delayed effect of radiation therapy. J Child Neurol. 1992;7:259-63. PMID: 1634747.

16 Fike JR, Sheline GE, Cann CE, Davis RL. Radiation necrosis. Prog Exp Tumor Res. 1984;28:136-51. PMID: 6484197.

17 Koike S, Aida N, Hata M, Fujita K, Ozawa Y, Inoue T. Asymptomatic radiation induced telangiectasia in children after cranial irradiation frequency latency and dose relation. Radiology. 2004;230:93-9. PMID: 14645879.

18 Lupo JM, Chuang CF, Chang SM, Barani IJ, Jimenez B, Hess CP, et al. 7-Tesla susceptibility-weighted imaging to assess the effects of radiotherapy on normal-appearing brain in patients with glioma. Int J Radiat Oncol Biol Phys. 2012;82:493-500. PMID: 22000750.

19 Oi S, Kokunai T, Ijichi A, Matsumoto S, Raimondi AJ. Radiation-induced brain damage in children--histological analysis of sequential tissue changes in 34 autopsy cases. Neurol Med Chir (Tokyo). 1990;30:36-42. PMID: 1694271.

20 Poussaint TY, Siffert J, Barnes PD, Pomeroy SL, Goumnerova LC, Anthony DC, et al. Hemorrhagic vasculopathy after treatment of central nervous system neoplasia in childhood: diagnosis and follow-up. AJNR Am J Neuroradiol. 1995;16:693-9. PMID: 7611024.